

Blends of poly(methyl methacrylate) with epoxy resin and an aliphatic amine hardener

Clara M. Gomez* and Clive B. Bucknall†

Cranfield Institute of Technology, Cranfield, Bedford MK43 0AL, UK
(Received 28 July 1992)

Miscibility, phase separation and curing behaviour have been studied in blends of poly(methyl methacrylate) (PMMA) with diglycidyl ether of bisphenol A (DGEBA) resin and 4,4'-diamino-3,3'-dimethyldicyclohexylmethane (3DCM) hardener. Quasi-binary mixtures of PMMA with the resin monomer show complete miscibility over the whole composition range, at all temperatures studied (-25 to 200°C). However, PMMA is much less miscible with the hardener, and cast films show two T_g values. Several techniques have been used to monitor phase separation and curing characteristics in PMMA blends, including viscometry, size exclusion chromatography, turbidity and optical microscopy. The morphologies and the thermal and dynamic mechanical properties of the cured blends, including non-stoichiometric compositions, are related to these observations.

(Keywords: poly(methyl methacrylate); epoxy resins; miscibility; stoichiometry; blends; morphology)

INTRODUCTION

Interactions between liquid epoxy resin monomers and dissolved polymers are important in determining the morphology and mechanical properties of the cured two-phase blends. The most extensive studies have been on solutions of CTBN (carboxyl-terminated poly(butadiene-co-acrylonitrile)) in DGEBA (diglycidyl ether of bisphenol A)¹⁻⁶, but there is also a growing body of literature on epoxy resin blends containing ductile thermoplastics, including polysulfones^{7,8} and poly(ether imides)⁹. Both elastomers and ductile thermoplastics can provide effective toughening if incorporated correctly into the resin.

For the present study, PMMA (poly(methyl methacrylate)) was chosen as a model additive, although no toughening effects are to be expected. The reasons for choosing PMMA were its solubility in the liquid epoxy resin, its phase separation during subsequent cure, and the position of its glass transition, which distinguishes it from the α and β relaxations of the cured resin. The results throw valuable light upon resin-polymer interactions, and upon phase separation during cure in epoxy resin blends at temperatures below or just above the T_g of the polymeric modifier.

The resin system was chosen in consultation with Professors J. P. Pascault and H. Sautereau, of INSA, Lyon, who have made a thorough study of CTBN blends based on the same epoxy-hardener combination⁴⁻⁶. The epoxy resin is almost pure DGEBA, and therefore forms a satisfactory basis for thermodynamic analysis of solubility characteristics, whilst the liquid aliphatic hardener allows the curing reaction to be carried out over a wide range of temperatures from 23°C upwards.

* Present address: Departamento Quimica-Fisica, University of Valencia, Doctor Moliner 50, Valencia, Spain

† To whom correspondence should be addressed

EXPERIMENTAL

Materials

The epoxy resin used was Dow DER332, a DGEBA having $M_n = 349 \text{ g mol}^{-1}$ and an average of 0.015 secondary hydroxyl groups per epoxy group. The hardener was BASF Laromin C260, which is 4,4'-diamino-3,3'-dimethyldicyclohexylmethane (3DCM). The thermoplastic modifier was ICI Diakon MG102, an injection-moulding grade of poly(methyl methacrylate) with $M_n = 28\,270$ and polydispersity $M_w/M_n = 1.98$, as measured by chromatography with polystyrene standards.

Initial miscibility

Initial miscibilities, in both hardener/PMMA mixtures and resin/PMMA mixtures, were studied by preparing 5 wt% solutions of individual components in methylene chloride, and mixing at room temperature. All hardener/PMMA blends, and those epoxy blends containing >20 wt% PMMA, were cast onto glass microscope slides: the resulting films were held for ≈ 4 days at 23°C until they reached constant weight. Blends containing 2–20 wt% PMMA, which were viscous liquids, were kept in a shallow glass dish throughout: for these blends, most of the solvent was removed under vacuum at 80°C .

These samples were quenched and held at -50°C for 5 min, before being tested in a Perkin-Elmer DSC4 differential scanning calorimeter at a heating rate of $10^{\circ}\text{C min}^{-1}$, to 150°C . In order to check reproducibility, the procedure was repeated a further two or three times. The temperature of onset of the transition was taken as T_g .

Infra-red spectra for neat components and mixtures were obtained using a Philips PU9600 FTi.r. instrument. Refractive indices were measured using an Abbé refractometer.

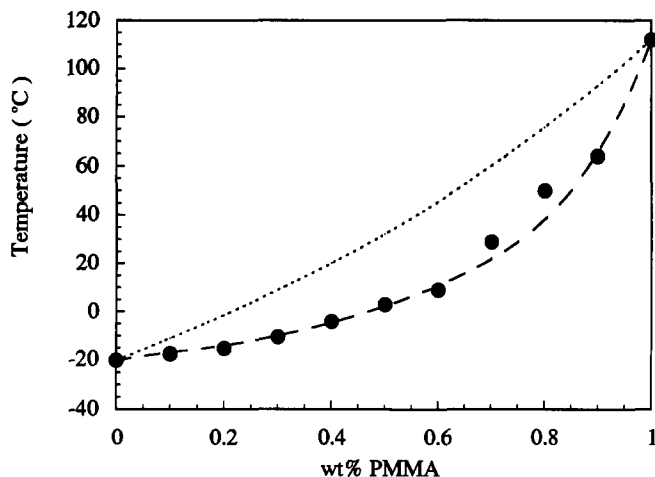


Figure 1 Relationship between T_g (from d.s.c.) and composition in quasi-binary mixtures of DER332 DGEBA and PMMA: (---) equation (1), with $\kappa = 0.20$; (.....) equation (2)

Cured blends

In making cured blends, PMMA beads were first dried at 80°C under vacuum for 24 h before being dissolved in methylene chloride at a concentration of 10 wt%. The resin was mixed with the stirred PMMA solution at room temperature, and stirring was continued until the solution was homogeneous. It was then heated in an oil bath to 80°C in order to drive off as much solvent as possible, the remainder being removed under vacuum at the same temperature over 14 h. A clear solution was obtained, which was then blended at 80°C with 3DCM. The main series of experiments were carried out on blends containing the stoichiometric amount of 3DCM (34.2 phr). Resin and 3DCM in the same proportions were also blended directly at 80°C to make control 'neat resin' samples. In addition, tests were carried out on mixtures having non-stoichiometric epoxy/hardener ratios r . Unless otherwise stated, the results presented below refer to resins with $r = 1$. The concentrations of PMMA quoted in this paper are calculated as mass fractions in the final blend.

For studies of the cloud point, resin and blend samples were cast into preheated parallel-plate glass moulds with a separation of 3 mm. Optical fibres were used to transmit light from a tungsten-halogen lamp through the heated cell to a Philip Harris i.r./light detector, and phase separation was observed through the decrease in transmitted light. Simultaneously, embedded thermocouples recorded resin temperatures.

Changes in gel fraction and T_g with increasing cure time under isothermal conditions were determined by casting samples into shallow aluminium pans and removing them from the oven at intervals. Samples were quenched in liquid nitrogen, ground to a powder, and weighed before and after extraction with methylene chloride. Gelation times were determined by extrapolating back to zero gel fraction. Part of each ground sample was used to determine T_g in the d.s.c. with a nitrogen atmosphere and a heating rate of 10°C min⁻¹. Onset values of the transition were used to characterize T_g . Vitrification time was defined as the point at which the T_g of the sample reached the cure temperature.

Viscosity changes during isothermal cure were monitored at a shear rate of 100 s⁻¹ in a coaxial-cylinder viscometer, the Contraves Rheomat 115. Experiments to

follow changes in the molecular weight of the curing resin were carried out at INSA, Lyon, using the size exclusion chromatography technique described by Verchère *et al.*⁵, with tetrahydrofuran (THF) as elution solvent.

Specimens for morphology studies were cast into 200 × 200 × 6 mm³ aluminium moulds coated with polytetrafluoroethylene (PTFE) and cured at one of five cure temperatures: 23, 50, 75, 100 and 120°C. Cure times, which were chosen to allow phase separation and gelation in the blends, were 6 days, 360 min, 100 min, 50 min and 30 min respectively. All plaques were post-cured for 14 h at 190°C.

The morphology of the cured blends was examined using both transmission electron microscopy of ultrathin sections and scanning electron microscopy of etched fracture surfaces. Sections for TEM were made on a Reichert-Jung Cryotome equipped with a diamond knife. Samples for SEM were broken in three-point bending at 23°C, immersed in methylene chloride for 2 h to dissolve exposed PMMA, and coated with gold/palladium. The electron micrographs were analysed using a Joyce-Loebl image analyser with Genias 2.5 software.

Dynamic mechanical tests were carried out at 10 Hz in a Polymer Laboratories DMTA machine, at a heating rate of 3°C min⁻¹.

RESULTS AND DISCUSSION

Binary DGEBA/PMMA blends

Binary blends of PMMA with DGEBA resin exhibited a single glass transition, as shown in Figure 1, indicating complete miscibility over the entire composition range. Further evidence for miscibility was obtained by holding mixtures containing 2 to 20 wt% PMMA in DGEBA at temperatures between -25 and 200°C. No turbidity was observed over this range. This contrasts with other DGEBA/polymer blends, which exhibit upper or lower critical solution temperature (UCST or LCST) behaviour.

The T_g data from d.s.c. measurements are compared in Figure 1 with the predictions of two equations relating the T_g of a miscible binary polymer to the weight fractions w_1 and w_2 of its components. The best fit is obtained from the Gordon-Taylor equation¹⁰:

$$T_g = \frac{w_1 T_{g1} + \kappa w_2 T_{g2}}{w_1 + \kappa w_2} \quad (1)$$

with the adjustable parameter κ assigned a value of 0.20. This low positive value of κ indicates attractive forces between PMMA and DGEBA, which are relatively weak in comparison with blends of polycaprolactone with chlorinated hydrocarbon polymers ($\kappa = 0.26, 0.51$ and 1.00 at 36, 56 and 67.2 wt% of chlorine¹¹) or of poly(vinyl chloride) (PVC) with poly(*n*-amyl methacrylate)¹² ($\kappa = 1.43$). A less successful fit is obtained from the Fox equation¹³:

$$\frac{1}{T_g} = \frac{w_1}{T_{g1}} + \frac{w_2}{T_{g2}} \quad (2)$$

which assumes zero enthalpic interaction. Strong interactions between specific chemical groups in miscible polymer blends cause detectable shifts in the relevant infra-red absorption peaks. In the case of PMMA, Kwei¹⁴ has reported a shift in the carbonyl peak from

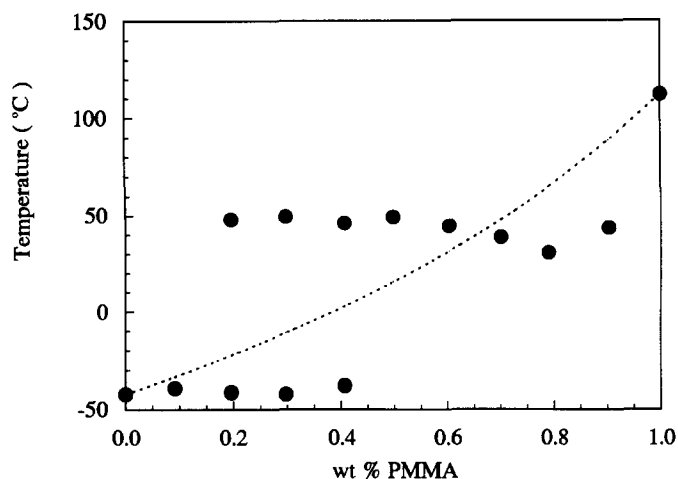


Figure 2 Relationship between transition temperatures (from d.s.c.) and composition in quasi-binary mixtures of 3DCM hardener and PMMA, showing evidence of phase separation: (.....) equation (2)

1722 to 1705 cm^{-1} on blending with Novolac resins. For this system, the interactions were so strong that it was necessary to add an additional term, in w_1w_2 , to the equations relating T_g to composition. By contrast, in the present work, blends containing 80 or 90 wt% DGEBA showed a shift of only 5 cm^{-1} in the wavenumber of the same peak. This supports the conclusion reached earlier on the basis of the low κ value that interactions between PMMA and DGEBA are positive but relatively weak.

Binary hardener/PMMA blends

Binary blends of PMMA with 3DCM hardener exhibit completely different behaviour. Over most of the composition range, there are two distinct transitions in the d.s.c. curve, as shown in Figure 2. The lower transition, at $\approx -40^\circ\text{C}$, is seen at PMMA concentrations up to 60 wt%, and coincides with the T_g of neat 3DCM. The upper transition, which lies between 40 and 50°C, clearly indicates the presence of a separate PMMA-rich phase containing a relatively small amount of 3DCM. This acts as a plasticizer, lowering the T_g of PMMA from its value (by d.s.c.) of 110°C for the neat polymer. From Figure 2, it appears that only about 10 parts of 3DCM in 90 parts of PMMA are required to bring the T_g down to 50°C.

Solubility parameter δ is a poor indicator of these differences in miscibility. Calculations using Fedors' method¹⁵ give δ (in $(\text{MJ m}^{-3})^{1/2}$) as 19.19 for PMMA, 19.39 for 3DCM, and 21.40 for DGEBA. The experimental results indicate that PMMA/3DCM mixtures are affected by strong molecular interactions that are not taken into account in the simple solubility parameter approach, which is based on a mean-field principle.

A comparison of the FTIR spectra for neat 3DCM hardener with corresponding spectra for PMMA and for 3DCM/PMMA blends provides evidence of strong interactions, presumably involving hydrogen bonding. Figure 3 shows the region of the N-H stretching modes of the primary amine groups in 3DCM. The band due to the asymmetric stretching mode shifts from 3363 cm^{-1} in neat 3DCM to 3376 cm^{-1} in a blend containing 90 wt% PMMA, whilst the band due to symmetric stretching shifts from 3286 to 3313 cm^{-1} . Since hydrogen

bonding increases interatomic spacings in the hydrogen-bearing molecule (N-H bond lengths in this case), thereby reducing vibration frequencies, it can be concluded from the FTIR data that hydrogen bonding is stronger between pairs of NH_2 groups in neat 3DCM than it is between NH_2 and $>\text{C}=\text{O}$ groups in 3DCM/PMMA blends. There is no detectable change in the carbonyl frequency. In the light of this evidence, it is proposed that the limited solubility of PMMA in 3DCM is due to strong self-association of the hardener rather than a lack of interactions between 3DCM and PMMA. In a diamine, hydrogen bonding could lead to self-association into large chain-like groups of molecules, whereas in monoamines interactions are more likely to be restricted to pairs of molecules.

Ternary epoxy/hardener/PMMA blends

Ternary blends were made by mixing the stoichiometric ratio of resin and hardener with 2, 5, 7 or 10 wt% PMMA. Isothermal curing experiments were carried out at temperatures between 50 and 150°C. The blends were initially transparent, but became turbid during the cure reaction. From Abbé refractometer data at 23°C, the refractive index n of PMMA is 1.489, whereas DGEBA and 3DCM have $n = 1.569$ and 1.499 respectively. Cloud-point times, t_{cp} , defined at the intercept between tangents to the curve at 0% and 50% loss of transmission, occur only a little before gelation and vitrification, showing that phase separation does not begin until the resin reaction is well advanced.

Over the range 2 to 10 wt% PMMA, concentration

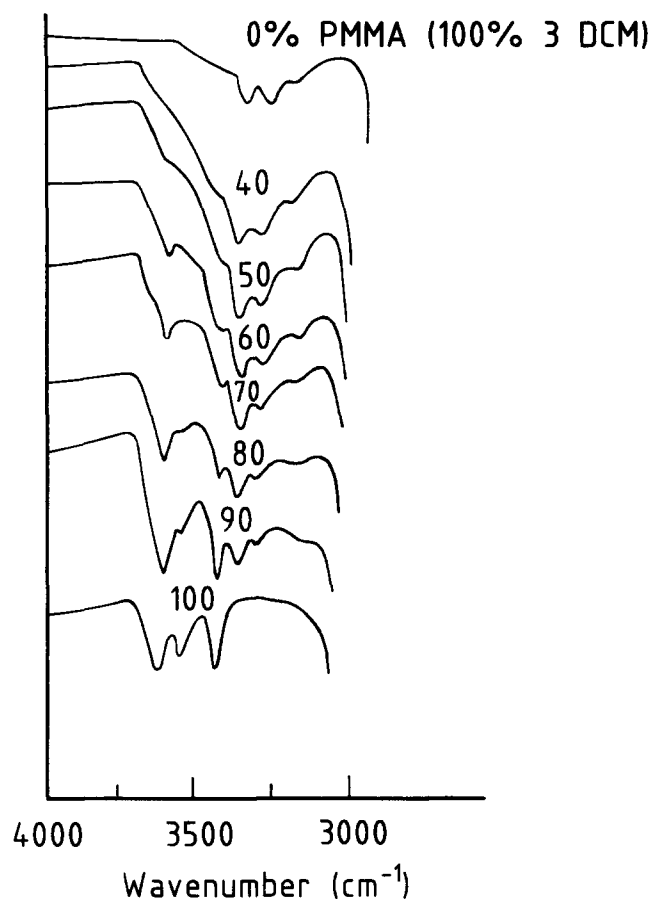


Figure 3 Details from FTIR spectra of PMMA, 3DCM and blends containing 40-90% PMMA

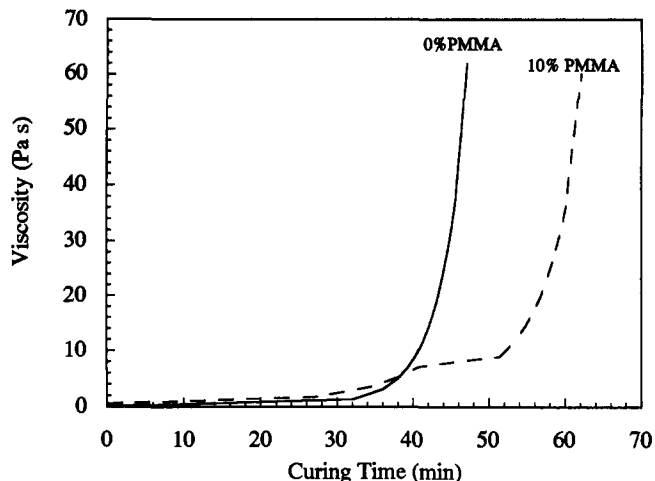


Figure 4 Viscosity changes in neat resin and blend containing 10% PMMA cured at 75°C. Shear rate = 100 s⁻¹

has little effect upon t_{cp} . Experiments with another PMMA of higher molecular weight ($M_n = 41\,540$, $M_w/M_n = 2$) gave identical cloud-point times. Arrhenius plots of $\log t_{cp}$ against T^{-1} gave $\Delta H = 41\text{ kJ mol}^{-1}$ for the curing reaction, which is in good agreement with the value of $\Delta H = 46\text{ kJ mol}^{-1}$ obtained by Montarnal *et al.*¹⁶ for the same resin with MNDA (1,8-diamino-*p*-menthane) in the presence of dissolved CTBN rubber.

Viscosity data at 75°C for the neat resin and a blend containing 10% PMMA are presented in Figure 4. Initially the added PMMA raises viscosity, as expected when a long-chain polymer is dissolved in a liquid. However, as cure proceeds and the blend begins to phase-separate, its viscosity falls below that of the neat resin at the same cure time. These results show that PMMA delays the curing reaction, and that the formation of PMMA-rich droplets in the still-liquid resin leads to a fall in viscosity. The shear applied in the viscometer helps to break down the continuous PMMA-rich phase structure that can form in unstirred blends. At smaller PMMA concentrations, the curves are intermediate between those for resins containing 0% and 10% PMMA. Similar observations were made in experiments at 50 and 100°C.

Isothermal *TTT* (time-temperature-transformation) diagrams for the neat resin and for a blend containing 10 wt% PMMA are compared in Figure 5. They show the general pattern observed previously by Gillham¹⁷ and by Verchère *et al.*⁵ for epoxy resin systems containing CTBN rubbers. There is an increase in both gelation and vitrification times on adding PMMA to the resin, especially in the region of higher cure temperatures.

Gelation is delayed because PMMA reduces the rate of reaction between DGEBA and hardener. This is clearly demonstrated in Figure 6, at a PMMA concentration of only 7%. Delayed gelation has also been reported by Verchère *et al.*⁵ for epoxy/3DCM/CTBN blends, and was observed in the present programme in epoxy/poly(ether sulfone) blends¹⁸. Dilution effects are partly responsible for the reduced rates of reaction, but other factors (such as autocatalysis⁵) can also contribute to variations in rate. Vitrification times are determined not only by the degree of conversion of the resin, but also by the temperature of the curing reaction in relation to the T_g of the continuous phase. Under certain

conditions, the presence of PMMA can raise the principal T_g in the blend at a given stage of cure, thereby tending to reduce the vitrification time. However, this effect is small compared with the decrease in reaction rate. The overall result of adding PMMA is therefore to increase gelation times.

The evolution of morphology during phase separation is revealed in hot-stage microscopy experiments. At a PMMA concentration of 10%, the system first appears to form a co-continuous structure with a periodicity of $\approx 1\text{--}2\ \mu\text{m}$, as shown in Figure 7a for a 10% PMMA blend cured at 100°C. This is followed by an increase in the volume fraction of the epoxy-rich phase, and an increase in optical contrast as the compositions of the two phases diverge (Figure 7b). If the cure temperature is sufficiently high (e.g. 100°C), and viscosity therefore

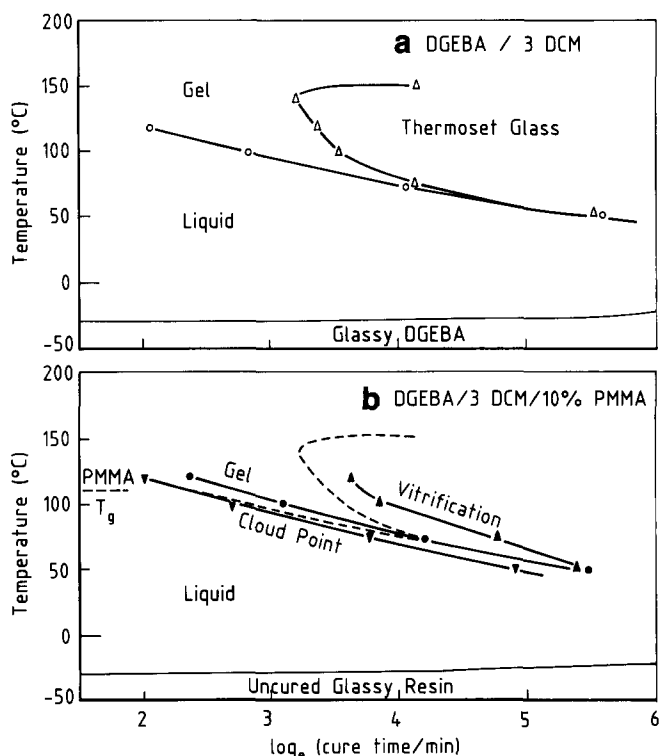


Figure 5 *TTT* diagram for (a) the neat resin, and (b) blends containing 10% PMMA. The broken curves in (b) show gelation and vitrification curves for neat resin, from (a)

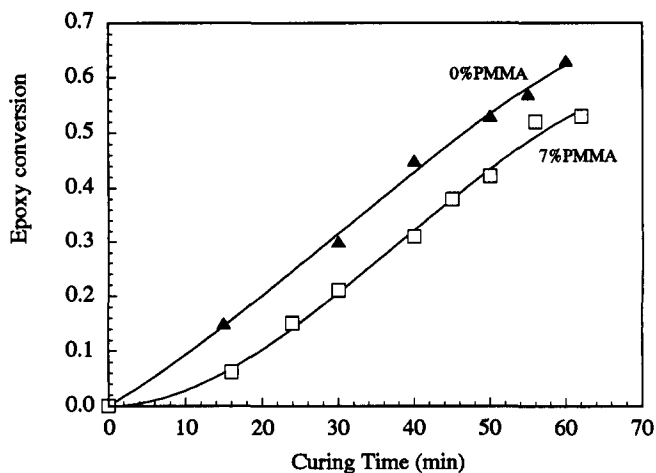


Figure 6 Kinetics of cure in neat resin and blend containing 7% PMMA cured at 75°C. Data from size exclusion chromatography

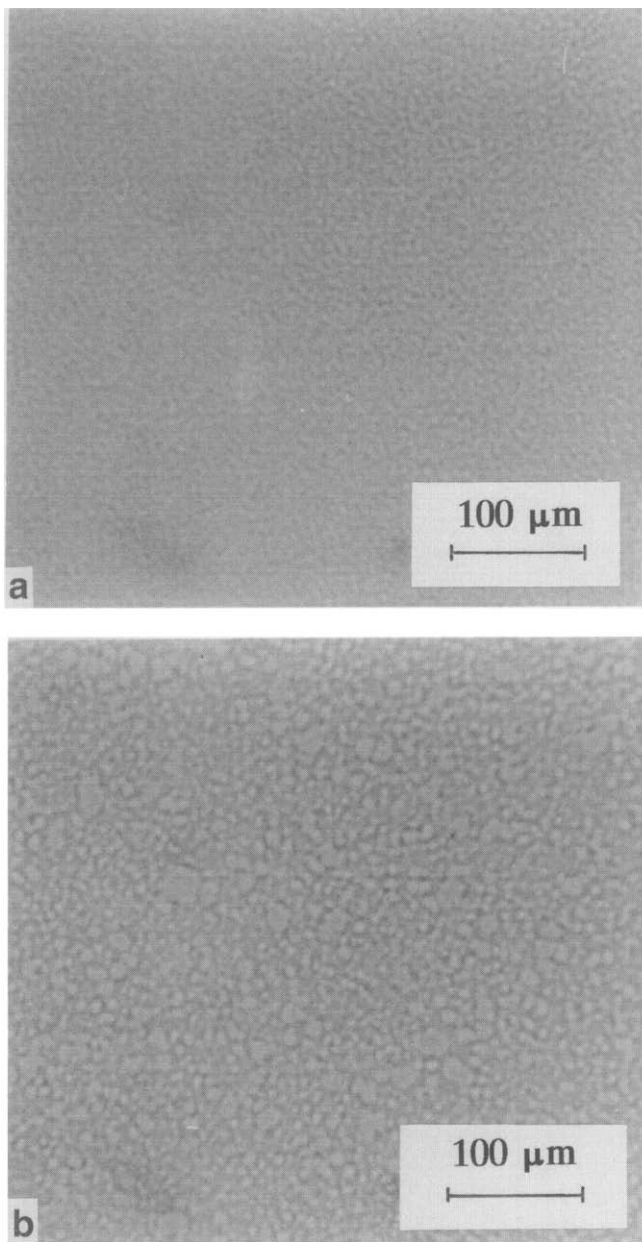


Figure 7 Optical micrographs of blend containing 10% PMMA cured at 100°C on a microscope hot stage for: (a) 12 min, (b) 30 min

low, the increase in interfacial tension then causes the PMMA-rich network to break up into large domains (as seen in Figure 7b), and eventually into individual small particles of PMMA. However, at lower temperatures, this process may be arrested by gelation and vitrification of the resin.

Cured stoichiometric compositions

The formation of a discrete PMMA phase is shown clearly in the dynamic mechanical data presented in Figure 8. There are four distinct peaks in the $\tan \delta$ curve: the β , ω and α peaks of the epoxy resin, at -41, 62 and 192°C respectively, and the α peak of the PMMA at 120°C. The positions of these peaks are essentially independent of cure temperature and PMMA concentration, within the range of the present experiments, as shown in Figure 9.

Figure 10 shows an ultramicrotomed section of a post-cured blend containing 10% PMMA, which was

cured initially at 75°C. In this material, the PMMA forms particles and domains ranging in size from <1 to >20 μm . The domains are irregular in shape and composite in structure, with prominent PMMA sub-inclusions. The size distribution of these sub-inclusions is striking: in the central region of a large PMMA domain, they are up to 2 μm across, whereas near the edges of a domain they tend to be very much smaller. These smaller sub-inclusions appear to be formed during

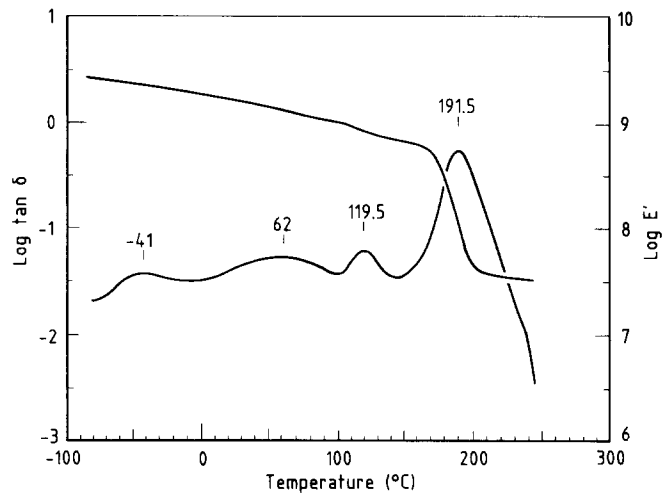


Figure 8 Dynamic mechanical loss curve for blend containing 10% PMMA, cured at 75°C

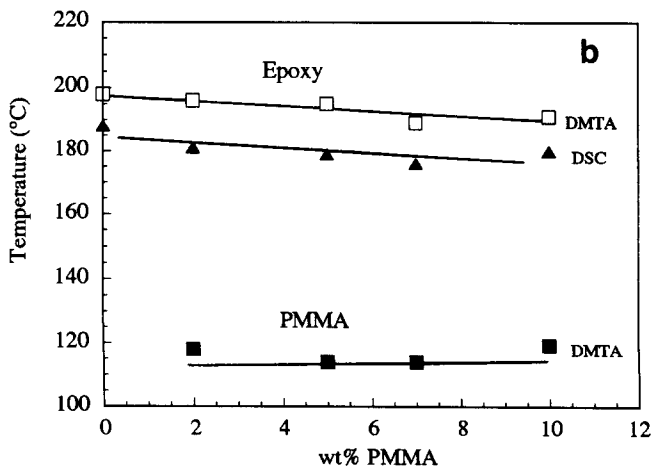
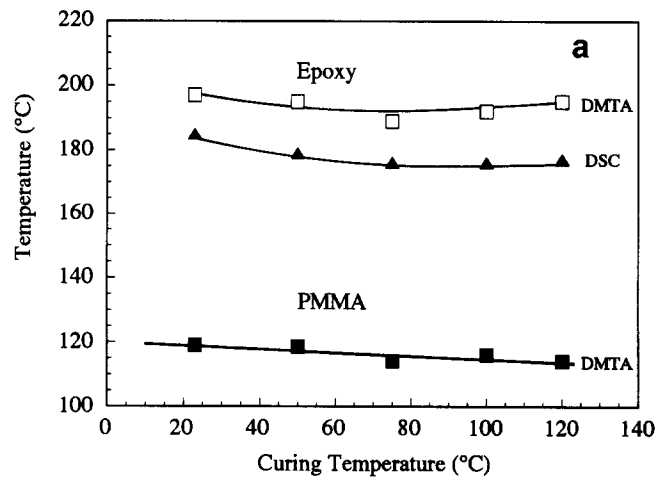


Figure 9 Effects of (a) cure temperature, and (b) PMMA concentration, on the T_g of fully cured plaques, from d.s.c. and d.m.t.a. data

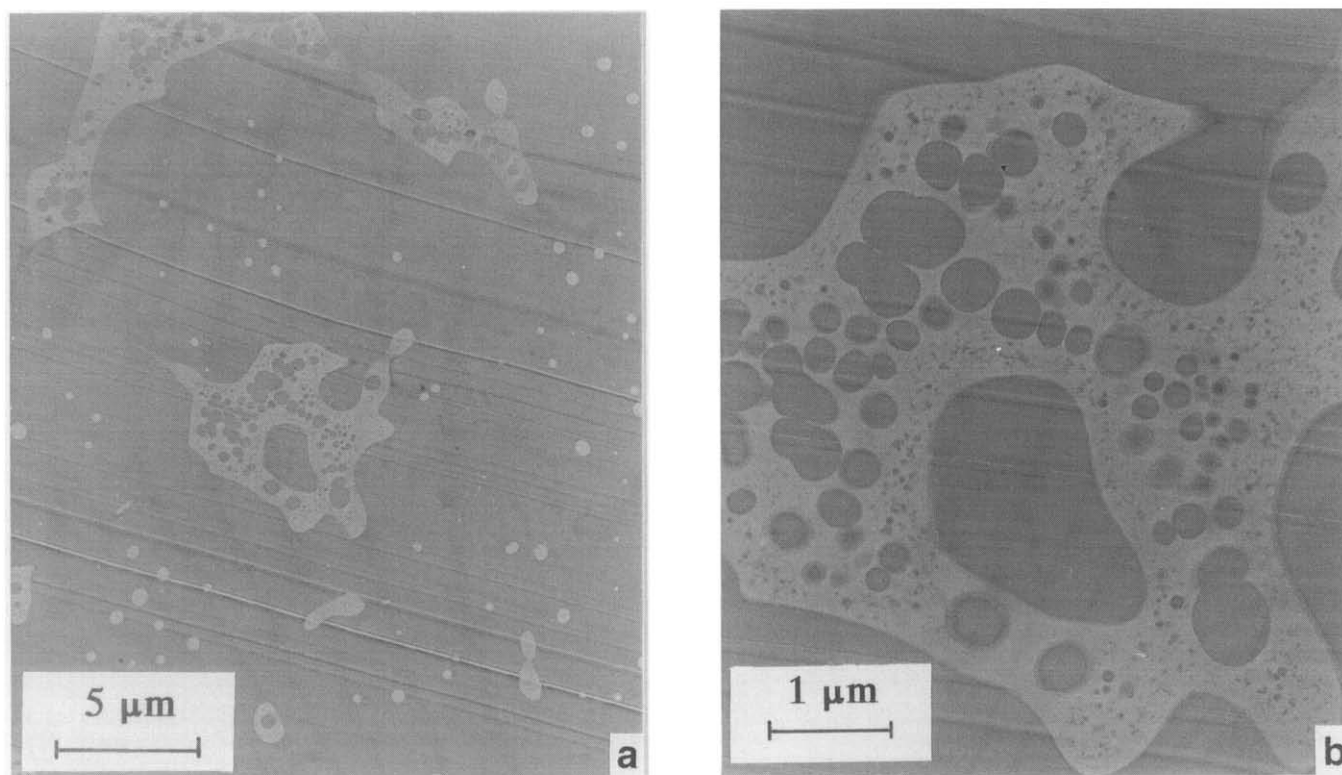


Figure 10 Thin section of blend containing 10% PMMA cured at 75°C: (a) general view; (b) detail of large domain, showing sub-inclusions

the later stages of phase separation, when increasing molecular weight causes a drop in the diffusion coefficient of the epoxy resin. Figure 10 illustrates the morphology that can develop from the networks shown in Figure 7a: the continuous PMMA-rich phase has broken down into discrete domains, and some individual particles have formed, but the process was arrested before all of the domains could divide into particles.

At 100 and 120°C, viscosities at the cloud point are lower, and the system remains more fluid whilst phase separation is taking place, with the result that the large domains formed at an early stage of the process break down to form spherical particles under the action of interfacial tension forces. Number-average domain diameters therefore decrease with increasing cure temperature, as shown in Figure 11. This result contrasts with observations on epoxy/CTBN^{1,6} and epoxy/polyoxypropylene¹⁹ blends, which show an increase in particle size with increasing cure temperature.

Post-curing at 190°C produces further small but detectable changes in morphology and domain sizes, as shown in Figure 11. At the beginning of post-cure, where the degree of conversion in the resin is about 80%, some diffusion is still possible at 190°C, since both the PMMA and the epoxy resin are well above their respective T_g values. Under these conditions, particles and domains that are close together can coalesce, with the result that the number of particles per unit volume decreases, and their diameters increase.

Cured non-stoichiometric blends

Figure 12 shows the effects on the α relaxation of the epoxy resin of deviating from r , the stoichiometric epoxy/hardener ratio. In both the neat resin and in blends containing PMMA, T_g falls when there is an excess

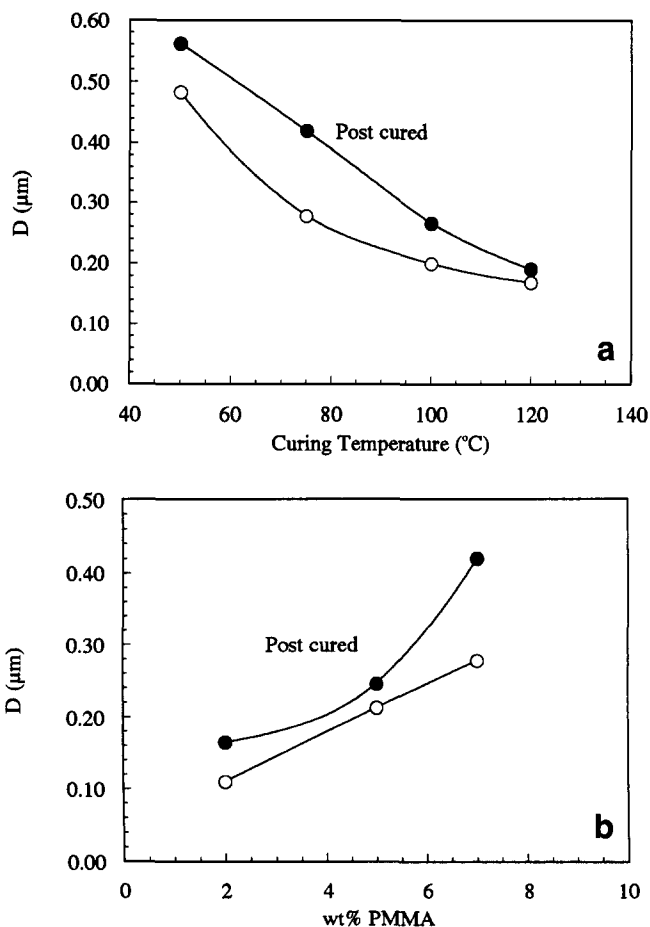


Figure 11 Effects on number-average diameter of PMMA particles/domains of varying: (a) cure temperature of 7% PMMA blend; and (b) PMMA content at cure temperature of 75°C. Data from SEM. Points: (○) before post-cure; (●) after post-cure at 190°C

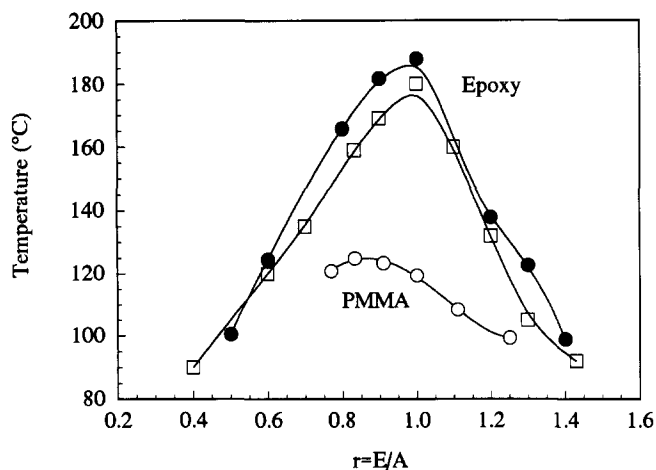


Figure 12 Effects of overall stoichiometric ratio on the T_g values of resin and PMMA phases. Blends cured at 75°C and post-cured at 190°C. Points: (○) T_g from d.m.t.a. in PMMA phase of blend containing 10% PMMA; (●) T_g from d.s.c. in neat epoxy resin; (□) T_g from d.s.c. in epoxy resin phase of 10% PMMA blend

of amine or epoxy groups. A similar result was reported by Galy *et al.*²⁰ for a range of neat epoxy resins with various hardeners.

Dynamic mechanical tests show that r also affects the α transition of the PMMA phase, which at $r = 0.86$ reaches a maximum of 126°C, the temperature of the d.m.t.a. α peak in neat PMMA. These results suggest that, at stoichiometric ratios above 0.86, the PMMA phase contains a small amount of residual unreacted DGEBA, which acts as a plasticizer. This was confirmed by Soxhlet extraction with THF of PMMA blends having $r = 1$, followed by size exclusion chromatography on the extract: small quantities of DGEBA were detected. From Figure 1, the amount of DGEBA required to reduce the T_g of PMMA by 10°C is of the order of 1–2%. For $r < 0.86$, the PMMA phase presumably contains excess 3DCM hardener.

The shift in maximum T_g for PMMA to $r = 0.86$ can be explained in terms of the differences in solubility of DGEBA and 3DCM. As a result of these differences, the concentration of 3DCM in the PMMA phase will be less than the stoichiometric ratio when the overall value of r in the blend is 1.0. Consequently, the excess DGEBA molecules in the PMMA phase must either diffuse to an interface with the resin, where they can react with hardener, or remain in the PMMA and lower its T_g . Only by reducing the overall r ratio can the amounts of DGEBA and 3DCM in the PMMA phase be adjusted to the stoichiometric ratio, so that the DGEBA can react to form longer chains (which have little effect on T_g) without having to diffuse to the boundary.

CONCLUSIONS

This work has shown that discussions of miscibility between liquid epoxy resins and thermoplastic additives should not be restricted to quasi-binary mixtures of the epoxy monomer with the polymeric additive: interactions with the hardener can give very different effects. In the

present instance, PMMA is quite soluble in liquid DGEBA resin, but not in 3DCM hardener.

The addition of PMMA has a marked effect on cure kinetics in the DGEBA/3DCM resin system. Rates of reaction are reduced by 25–30%, with the result that gelation and vitrification times are significantly increased. Cured blends can develop a complex morphology, especially at lower cure temperatures, where they form large PMMA domains containing resin sub-inclusions of various sizes. At higher temperatures, blends tend to form discrete small particles, provided that the PMMA concentration is not too high. An interesting new observation is that further, albeit minor, changes in morphology can occur during post-curing.

Finally, the work has shown that the T_g of the PMMA phase depends upon the stoichiometric epoxy/hardener ratio in the blend. Surprisingly, the maximum PMMA T_g occurs at a stoichiometric ratio $r = 0.86$. This can be explained by the differences in solubility between DGEBA resin and 3DCM hardener.

ACKNOWLEDGEMENTS

The authors thank the Science and Engineering Council for a grant in support of this work (GR/F/18404). The study forms part of a collaborative programme with INSA, Lyon, and valuable discussions with Professor J. P. Pascault and H. Sautereau are gratefully acknowledged.

REFERENCES

- Butta, E., Levita, G., Marchetti, A. and Lazzeri, A. *Polym. Eng. Sci.* 1986, **26**, 63
- Vazquez, A., Rojas, A. J., Adabbo, H. E., Borrajo, J. and Williams, R. J. J. *Polymer* 1987, **28**, 1156
- Lee, W. H., Hodd, K. A. and Wright, W. W. *Adv. Chem. Ser.* 1989, **222**, 263
- Verchère, D., Sautereau, H., Pascault, J. P., Moschiar, S. M., Riccardi, C. C. and Williams, R. J. J. *Polymer* 1989, **30**, 107
- Verchère, D., Sautereau, H., Pascault, J. P., Moschiar, S. M., Riccardi, C. C. and Williams, R. J. J. *J. Appl. Polym. Sci.* 1990, **41**, 467
- Verchère, D., Sautereau, H., Pascault, J. P., Moschiar, S. M., Riccardi, C. C. and Williams, R. J. J. *J. Appl. Polym. Sci.* 1991, **42**, 701
- Yamanaka, K. and Inoue, T. *Polymer* 1989, **30**, 662
- Hedrick, J. L., Yilgor, I., Jurek, M., Hedrick, J. C., Wilkes, G. L. and McGrath, J. E. *Polymer* 1991, **32**, 2020
- Bucknall, C. B. and Gilbert, A. H. *Polymer* 1989, **30**, 213
- Gordon, M. and Taylor, J. S. *J. Appl. Chem.* 1952, **2**, 493
- Hubbell, D. S. and Cooper, S. L. *J. Appl. Polym. Sci.* 1977, **21**, 3035
- Perrin, P. and Prud'homme, R. E. *Polymer* 1991, **32**, 1468
- Fox, T. G. *Bull. Am. Phys. Soc.* 1956, **1**, 123
- Kwei, T. K. *J. Polym. Sci., Polym. Lett. Edn.* 1984, **22**, 307
- Fedors, R. F. *Polym. Eng. Sci.* 1924, **14**, 142
- Montarnal, S., Pascault, J. P. and Sautereau, H. *Adv. Chem. Ser.* 1989, **222**, 193
- Chan, L. C., Gillham, J. K., Kinloch, A. J. and Shaw, S. J. *Adv. Chem. Ser.* 1984, **208**, 235
- Bucknell, C. B., Gomez, C. M. and Quintard, I. *Polymer* submitted
- Korkakos, G., Gomez, C. M. and Bucknall, C. B. *Plast. Rubb. Compos. Process. Applic.* in press
- Galy, J., Sabra, A. and Pascault, J. P. *Polym. Eng. Sci.* 1986, **26**, 1514